Use of Describing Functions for Predicting Low-Loss AMB Performance

Kenneth Diemunsch and Panagiotis Tsiotras

Abstract— **Active Magnetic Bearings (AMBs) offer an alternative to conventional ball bearings. Their main advantages stem from the lack of physical contact between the rotor and the stator, and their potential for active disturbance rejection. AMBs are indispensable for high-speed electromechanical flywheel batteries, which have been proposed recently as a replacement of chemical batteries on-board orbiting satellites. In order to be competitive with chemical batteries, these flywheel batteries must operate at very high speeds and have low dissipative losses. Low-losses imply AMB operation in low flux or current bias. In this paper we analyze the disturbance rejection properties of a recently proposed low-bias AMB controller subject to an imbalance force. We use describing functions to analyze and predict the magnitude of position oscillations of the AMB under the imbalance force.**

I. INTRODUCTION

Bearings are primary components of all rotating machinery. Their role is to support the rotating shaft (the rotor) inside the stator. Active magnetic bearings (AMBs), in particular, have many advantages over conventional (mechanical) ball bearings. Their main advantage is their frictionless operation due to lack of contact between the rotor and the stator. Their potential to provide high-speed, frictionless operation and active disturbance rejection makes AMBs ideal candidates for several industrial applications. In fact, AMBs have been successfully used in various applications such as vacuum pumps, hard-disk drives, high-speed centrifuges, flywheels, high-speed turbines, and machine tools [1], [2], [3], [4], [5].

AMBs are indispensable for the recently proposed high-speed electromechanical flywheel batteries, which have been promoted as a light-weight alternative to replace chemical batteries on-board orbiting satellites [2], [6], [7]. To be competitive with chemical batteries, these flywheel batteries need to operate at very high-speeds (on the order of 60-80K rpm). Achieving efficient operation at such speeds requires minimization of mechanical, electrical and other losses. Since AMBs are frictionless, they do not suffer from mechanical losses. Electromagnetic (e.g., eddy current, ohmic) losses on the other hand, are still present. These are proportional to the total flux of the bearings. Minimization of the flux is thus essential for designing efficient AMBs for flywheel batteries.

K. Diemunsch, graduate student, D. Guggenheim School of Aerospace Engineering, Georgia Institute of Technology, Atlanta, GA 3032-0150, USA. E-mail: kenneth.diemunsch@gmail.com

P. Tsiotras, Associate Professor, D. Guggenheim School of Aerospace Engineering, Georgia Institute of Technology, Atlanta, GA 3032-0150, USA. E-mail: p.tsiotras@ae.gatech.edu

The force generated by an electromagnetically active bearing is a nonlinear function of the flux (or current). It is customary to linearize the force/flux characteristic by introducing a flux (or current) bias. Since electromagnetic losses are proportional to the total flux, it is of primary importance for flywheel batteries to operate at a very small (or zero) flux bias. Complete elimination of the flux bias however results in a linearly uncontrollable system. Moreover, controllability is reduced as the bias flux (or current) tends to zero. Thus, nonlinear techniques are required to control AMBs at zero or low bias. In [8] several control designs were proposed to allow operation of an AMB at zero or low bias flux. No analysis of the AMB under imbalance forces was attempted in [8], however. AMBs are always subjected to imbalance forces due to the fact that the center of mass of the shaft is never perfectly aligned with the axis of rotation. In this paper, we propose a method to predict the imbalance disturbance rejection performance of a low-loss AMB using describing function theory. Specifically, we use describing functions to quasi-linearize the equations, and we propose a method for choosing the controller gains in order to achieve the desired performance (in terms of shaft deflection) while minimizing the magnitude of the flux.

II. THE AMB MODEL AND CONTROL DESIGN

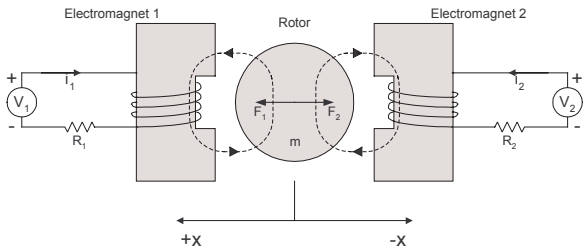

Fig. 1. Schematic of a 1-DOF AMB.

We consider a (1-DOF) AMB as shown in Fig. 1. The AMB consists of two electromagnets, which are used to move a mass m in one dimension. It is assumed that all motion takes place in the x direction and that gravity is not present. The control design uses the voltage inputs to the electromagnets, V_1 and V_2, in order to vary the forces acting on the mass. Since an electromagnet can only produce an attractive force, two electromagnets are required to generate forces in both the positive and negative x directions.

Let Φ_i, denote the total flux through the i-th electromagnet ($i = 1, 2$). The equation of motion of the mass is given

by

$$m\ddot{x} = \frac{1}{\mu_0 A_{\rm g}}(\Phi_1^2 - \Phi_2^2), \tag{1}$$

where m is the mass of the rotor, μ_0 is the permeability of free space (=1.25$\times 10^{-6}$H/m) and $A_{\rm g}$ is the area of each electromagnet pole. Let $\Phi_0 \geq 0$ denote the bias flux (assumed to be the same for both electromagnets). Then

$$\Phi_i = \Phi_0 + \phi_i \qquad i = 1, 2, \tag{2}$$

where ϕ_i is the control flux. To achieve low-bias operation, Φ_0 is typically small, and we activate only one electromagnet at a time. We thus implement the switching rule

$$\begin{aligned} V_1 = \nu, \quad V_2 = 0 \quad \text{when} \quad \phi \geq 0, \\ V_1 = 0, \quad V_2 = \nu \quad \text{when} \quad \phi < 0, \end{aligned} \tag{3}$$

where ϕ is the *generalized control flux*, defined as $\phi := \phi_1 - \phi_2$, and ν is the *generalized control voltage*. Hence, each time one of the coils generates the minimum possible flux (the flux bias), while only the *control flux* ϕ activates the other coil. The flux-dependent, voltage switching scheme in (3) is coined the *generalized complementary flux condition* (*gcfc*) [8]. It is shown in [8] that applying the complete equations can be written in non-dimensionalized form as follows

$$\dot{z}_1 = z_2, \tag{4a}$$
$$\dot{z}_2 = \varepsilon y + y|y|, \tag{4b}$$
$$\dot{y} = u, \tag{4c}$$

where $\varepsilon = 2\Phi_0/\Phi_{\rm sat}$. In (4) the first two equations are essentially a restatement of (1), where z_1 is non-dimensionalized position and z_2 is non-dimensionalized velocity. Equation (4c) is just Faraday's law where z_3 is the non-dimensionalized control flux and u is the corresponding non-dimensionalized control voltage[1].

It is shown in [8] that the control law

$$u(z_1, z_2) = -k_1 z_1 - k_2 z_2 - \gamma\eta, \tag{5}$$

where $k_1 > 0$, $k_2 > 0$, $\gamma > 0$, and $\eta := y + k_1 z_1 + k_2 z_2$, ensures global asymptotic stability about the origin for the system (4).

III. Imbalance Disturbance Force

If the center of mass of the rotor is not aligned with the axis of rotation, but rather it is located at a distance e from the geometrical center, then during operation a sinusoidal imbalance vibration results. This disturbance can be modeled by

$$w(\tau) = A \sin \omega\tau, \tag{6}$$

where $\omega := \Omega\sqrt{g_0\kappa}/\Phi_{\rm sat}$ is the non-dimensional speed of rotation, $A = e\omega^2/g_0$ and $\tau = t\Phi_{\rm sat}/\sqrt{g_0 m \mu_0 A_{\rm g}}$ is the non-dimensionalized time.

[1]For simplicity, in (4c) the voltage drop across the coil has been neglected.

Adding this unbalance disturbance to (4) and recalling that the maximum flux can never exceed $\Phi_{\rm sat}$ yields

$$\dot{z}_1 = z_2, \tag{7a}$$
$$\dot{z}_2 = \varepsilon\,{\rm sat}(y) + |{\rm sat}(y)|{\rm sat}(y) + w, \tag{7b}$$
$$\dot{y} = u. \tag{7c}$$

For notational simplicity, the function ${\rm sat}(\cdot)$ in (7b) denotes the saturation function with level $\delta := 1 - \Phi_0/\Phi_{\rm sat}$. This is owing to the fact that if the maximum level of the total flux $\Phi_0 + \phi_i$ in each electromagnet is $\Phi_{\rm sat}$, the maximum level of the control flux is $(\Phi_{\rm sat} - \Phi_0)/\Phi_{\rm sat}$.

IV. Quasi-linearization via Describing Functions

The controller (5) makes the system globally asymptotically stable for any $k_1 > 0$, $k_2 > 0$ and $\gamma > 0$, but we have no additional information on how to choose their values. For instance, it would be of importance for a control law comparison to have a method to choose the controller gains as a function of the desired disturbance rejection, avoiding trial and error.

Since imbalance is a sinusoidal function, in the sequel we use describing function analysis, to predict the imbalance deflection for any given values of the controller gains.

A. Describing Functions of the AMB Nonlinearities

In this section, we compute the describing function to replace the nonlinearities in (7b). Recall that this method, also called harmonic balance [9], [10], [11], is a type of quasi-linearization applied to nonlinear operators, and it is valid only for sinusoidal inputs. The describing function of a nonlinear function is obtained by applying a sinusoidal input to the nonlinearity and by computing the ratio of the Fourier transform coefficients of the first harmonic at the output. The describing function can be thought as an "equivalent gain" of a linear time-invariant element, whose response to $a\sin\omega t$ is $\Psi(a,\omega)\,a\sin\omega t$, where $\Psi(a,\omega)$ is the describing function.

The first nonlinearity that shows up in equation (7b) is

$$\psi_1(y) := |y|y, \tag{8}$$

where y is the control flux. This nonlinearity is time invariant and odd. It is known [12] that for an odd, time-invariant, memoryless nonlinearity, say $\psi(a\sin\theta)$, the corresponding describing function is given by

$$\Psi(a) = \frac{2}{\pi a}\int_0^\pi \psi(a\sin\theta)\sin\theta\,{\rm d}\theta. \tag{9}$$

Making use of (9) we may compute the associated describing function for (8) as follows

$$\Psi_1(a) := \frac{8a}{3\pi}. \tag{10}$$

Hence the output of $\psi_1(y) = |y|y$ when $y = a\sin\omega t$ can be approximated by $\frac{8a}{3\pi}a\sin\omega t$.

The second nonlinearity in (7b) is a the saturation function, which is a piecewise linear function. The saturation acts on the control flux y with saturation level δ. It can be shown that the corresponding describing function is

$$\Psi_2(a) := \begin{cases} 1\,, & \text{if } 0 \le a \le \delta, \\ \frac{2}{\pi}\Big(\sin^{-1}(\frac{\delta}{a}) + \frac{\delta}{a}\sqrt{1-(\frac{\delta}{a})^2}\Big)\,, & \text{if } a > \delta, \end{cases} \tag{11}$$

where δ is the non-dimensional maximum value of the control flux.

V. Application to the nonlinear AMB model

The controller in (5) has three tunable gains, namely, k_1, k_2 and γ. The gain γ plays a major role in tracking the desired control flux [8]. This gain has much less influence on the magnitude of the position oscillations than the controller gains k_1 and k_2. Hence, it is possible to decouple the mechanical and the electrical dynamics, and assume an instantaneous control flux implementation. The mechanical subsystem takes the form of the single-input, single-output nonlinear system

$$\ddot{z}_1 = \varepsilon \mathrm{sat}(y) + |\mathrm{sat}(y)|\mathrm{sat}(y) + w \tag{12a}$$
$$y = -k_1 z_1 - k_2 \dot{z}_1 \tag{12b}$$

with input w and output y.

Since superposition and commutativity does not hold for nonlinear operators, application of describing function theory to (12) requires the derivation of the describing function for the combined nonlinear term $|\mathrm{sat}(y)|\mathrm{sat}(y)$.

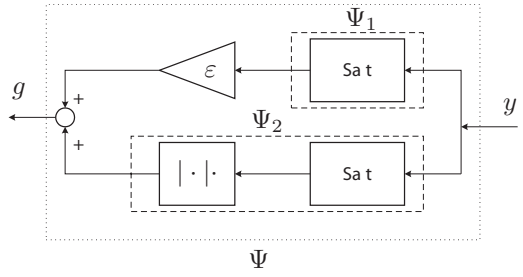

Fig. 2. Decomposition of the system nonlinearities.

To this end, consider the block-diagram representation of the rhs of (12a), shown in Fig. 2. Assuming $y = a\sin\omega\tau$, we want to find $\Psi(a)$ such that

$$\ddot{z}_1 = \varepsilon\,\mathrm{sat}(y) + |\mathrm{sat}(y)|\mathrm{sat}(y) + w = \Psi(a)y + w \tag{13}$$

where $\Psi(a)$ represents the describing function associated with the combined nonlinearity. To compute $\Psi(a)$, we use the describing function definition to write

$$\begin{aligned}\Psi(a) &= \varepsilon\frac{2}{\pi a}\int_0^{\pi} a\sin^2\theta\,\mathrm{d}\theta \\ &\quad + \frac{2}{\pi a}\int_0^{\pi} |a\sin\theta| a\sin\theta\sin\theta\,\mathrm{d}\theta.\end{aligned}$$

Note that in the first term, only the saturation is involved and it is scaled by the gain ε. From Fig. 2 one has that

$$\Psi(a) = \varepsilon\,\Psi_2(a) + \Psi_3(a) \tag{14}$$

where $\Psi_2(a)$ is the saturation function calculated earlier. The second part $\Psi_3(a)$ is the describing function of the combined nonlinearity $|\mathrm{sat}(y)|\mathrm{sat}(y)$.

We have already computed the describing function associated with the nonlinearity $|y|y$ when the control flux does not saturate. We therefore have that $\Psi_3(a) = \Psi_1(a) = 8a/3\pi$ when $0 \le a \le \delta$.

Let us now derive the expression of the describing function $\Psi_3(a)$ in the presence of saturation. An easy calculation shows

$$\begin{aligned}\Psi_3(a) &= \frac{4}{\pi a}\int_0^{\beta} a^2\sin^3\theta\,\mathrm{d}\theta + \frac{4}{\pi a}\int_{\beta}^{\frac{\pi}{2}} \delta^2\sin\theta\,\mathrm{d}\theta \\ &= \frac{4a}{\pi}\Big(-\frac{1}{3}\sin^2\beta\cos\beta - \frac{2}{3}\cos\beta + \frac{2}{3}\Big) + \frac{4\delta^2}{\pi a}\cos\beta\end{aligned}$$

where $\beta = \sin^{-1}(\delta/a)$. Substituting β in the previous expression, one obtains

$$\begin{aligned}\Psi_3(a) &= \frac{4a}{\pi}\Big(-\frac{1}{3}(\frac{\delta}{a})^2\sqrt{1-(\frac{\delta}{a})^2} - \frac{2}{3}\sqrt{1-(\frac{\delta}{a})^2} \\ &\quad + \frac{2}{3} + \frac{4\delta^2}{\pi a}\sqrt{1-(\frac{\delta}{a})^2}\Big).\end{aligned}$$

Finally,

$$\Psi_3(a) = \begin{cases} \frac{8a}{3\pi}, & \text{if } 0 \le a \le \delta, \\ \frac{8a}{3\pi}\,\Big(\sqrt{1-(\frac{\delta}{a})^2}\,\big[(\frac{\delta}{a})^2 - 1\big] + 1\Big), & \text{if } a > \delta. \end{cases} \tag{15}$$

VI. Performance Analysis

Let us assume that the non-dimensional control flux and position can be approximated by sinusoids of frequency ω and magnitude a and p, respectively. That is, assume

$$y(\tau) \simeq a\,\sin\omega\tau, \quad z_1(\tau) \simeq p\,\sin\omega(\tau+\theta). \tag{16}$$

Using the describing functions, in the Laplace domain the equations one obtains

$$Y(s) = \frac{H(s)G(s)}{1 - G(s)\Psi(a)H(s)}W(s). \tag{17}$$

where $H(s) = -k_1 - sk_2$ and $G(s) = 1/s^2$. Since we have assumed that the magnitude of control flux oscillations is a, the following constraint equation holds It follows that, given k_1 and k_2, the constraint

$$a^2 = \frac{k_1^2 + \omega^2 k_2^2}{(\Psi(a)k_1 - \omega^2)^2 + (\Psi(a)\omega k_2)^2}A^2 \tag{18}$$

relates a and A for each frequency ω. Moreover, we have the following relationship between the magnitude of the position oscillations and the magnitude of the control flux

$$Y(s) = (-k_1 - k_2 s)\,Z_1(s).$$

It follows that

$$a = (k_1^2 + \omega^2 k_2^2)^{\frac{1}{2}} p. \tag{19}$$

In summary, the magnitude of the imbalance A and the magnitude of the position oscillations p are related via (18) and (19). Hence, for a desired magnitude of position oscillations p, we can find the controller gains k_1 and k_2 that satisfy the constraint equation and ensure that the magnitude of position oscillations is close to the desired value p. The method will work provided all system states are sinusoids. This issue is investigated in Section VIII.

VII. Numerical Examples

Numerical examples have been performed to validate the proposed analysis. In the numerical simulations that follow we have used an AMB with the same specifications as in [13], [14]. These are shown in Table I.

TABLE I
AMB Specifications.

Symbols	Meaning
$N = 321$	# of turns in coil
$m = 4.5$ kg	effective mass of the rotor
$\Phi_{\rm sat} = 200\mu$Wb	saturation flux
$A_{\rm g} = 137$ mm^2	electromagnet pole area
$g_0 = 0.33$ mm	nominal width of airgap (when $x = 0$)
$e = 0.02$ mm	eccentricity

Case A: No Saturation

Let us use $k_1 = k_2 = 5$, a speed of rotation equal to 10,000 rpm ($\omega = 2.64$), and a flux bias of $\Phi_0 = 10\ \mu$Wb, resulting in $\varepsilon = 0.1$. One computes the value of a using (18), assuming no saturation. We get $a = 0.646$, which corresponds to a magnitude of oscillations of the control flux equal to 129 μWb. Using (19) we compute the expected value of the non-dimensional position oscillations. We get $p = 0.0458$, which corresponds to a magnitude of $p \times g_0 = 0.015$ mm. A numerical simulation, shown in Fig. 3, confirms that, with surprising precision, the magnitude of the control flux oscillations is 128 μWb and the magnitude of the position oscillations is 0.015 mm ($\gamma = 1$).

Case B: Saturation

Now let us assess the describing function method when both nonlinearities are present. Assume a desired magnitude of position oscillations equal to 0.030 mm ($p = 0.0909$) with a flux bias $\Phi_0 = 150\ \mu$Wb. The AMB is assumed to be operating at 15,000 rpm ($\omega = 3.97$). Fixing $k_2 = 1$, we want to find the controller gain k_1 that results in the desired magnitude of position oscillations. Using the constraint equation with saturation, we find $k_1 = 9.10$. The results from the numerical simulation of the system using these values, and imposing the saturation are shown in Fig. 4. The magnitude of position oscillations is 0.0295 mm, which is again very close to the desired magnitude of position oscillations.

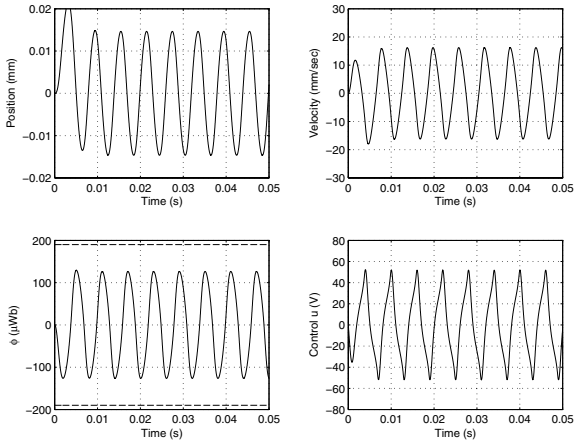

Fig. 3. Simulation of the AMB. Case without saturation ($\omega = 2.64$, $\varepsilon = 0.1$, $k_1 = k_2 = 5$, $\gamma = 1$).

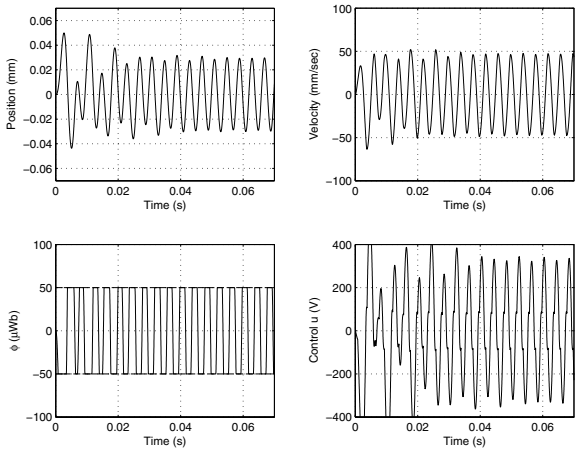

Fig. 4. Simulation of the AMB. Case with saturation ($\omega = 3.97$, $\varepsilon = 1.5$, $k_1 = 9.1$, $k_2 = 1$, $\gamma = 20$).

Note that for these simulations, the value of the gain γ was set to a larger value, $\gamma = 20$. Recall that our analysis of Section V implies that the control flux is implemented instantaneously and the speed of the implementation depends primarily on the parameter γ. When considering only the nonlinearity $|y|y$, our simulations have indicated that setting $\gamma = 1$ was sufficient. In the presence of saturation however, tracking of the desired flux seems to be more crucial, resulting in larger values of γ. Large values of γ, on the other hand, may lead to voltage saturation; see bottom right plot of Fig. 4. The issue of voltage saturation for low-bias AMBs has been addressed in [14].

VIII. Flux Optimization

In the previous section, we were able to choose the nonlinear controller gains k_1 and k_2 so that the actual magnitude of the position equaled a desired value. Note however, that there are many combinations of values of the gains k_1 and k_2 that yield the same desired position magnitude. It is natural to choose the pair associated with

the minimum magnitude of the control flux. Using (18) and (19) we may therefore set up an optimization problem to minimize the flux for the desired magnitude of the position oscillations.

To this end, consider the problem of minimizing $f(k_1, k_2) := k_1^2 + \omega^2 k_2^2$ subject to the equality constraint

$$C = \frac{k_1^2 + \omega^2 k_2^2}{(\Psi(a)k_1 - \omega^2)^2 + (\Psi(a)\omega k_2)^2} A^2 - a^2 = 0 \quad (20)$$

The optimization parameters are the controller gains k_1 and k_2, for given values of ω, ε, A, and p. An analytic solution to this problem is rather cumbersome. Instead, we can get a great deal of information by plotting the function to be minimized and the constraint equation in the (k_1, k_2) plane.

Figures 5-6 show the constraint in the (k_1,k_2) plane for different magnitudes of position oscillations and different speeds of rotation. The flux bias is chosen as $\Phi_0 = 10\mu$Wb. Superimposed on these plots are the level sets of the function f.

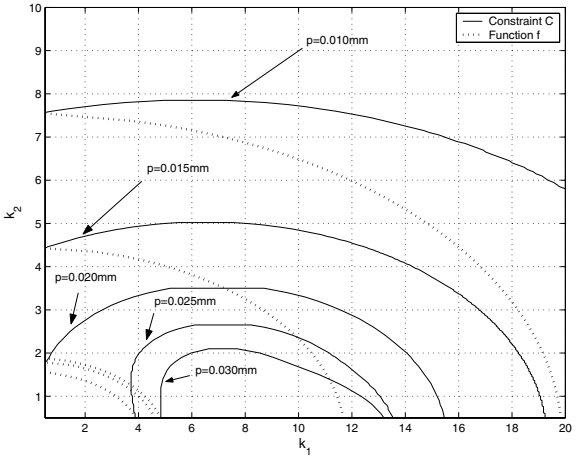

Fig. 5. Constraint for $\Omega = 10,000$ rpm ($\omega = 2.64$).

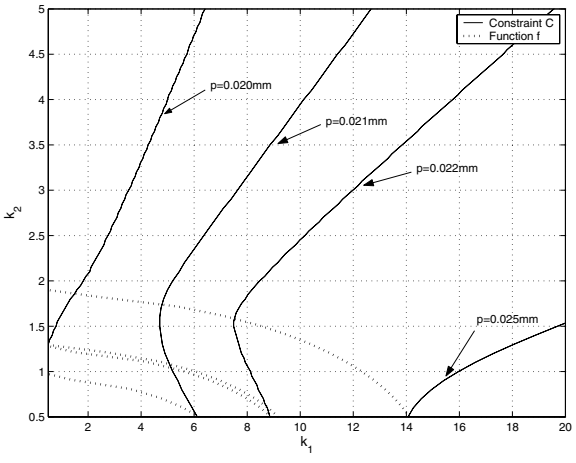

Fig. 6. Constraint for $\Omega = 30,000$ rpm ($\omega = 7.94$).

It follows from these plots that the minimum always occurs on one of the coordinate axes. Recall that one requires $k_1 > 0$ and $k_2 > 0$ for stability. Therefore, to find the controller gains that result in a given magnitude p, while at the same time minimizing the control flux, we pick the minimum allowable value of k_1 and find subsequently k_2 from the constraint equation. If no solution exists, we may alternatively pick the minimum allowable value of k_2 and compute k_1 from the constraint equation. If a solution exists for both cases, we may compute the value of f for both cases, and then pick the pair associated with the minimum value of f.

IX. Subharmonic Response

Recall that for the describing function analysis to be applicable, the input to the nonlinearity has to be a sinusoidal function. Our simulation results indicated that when k_1 and k_2 are small positive numbers the states may not be necessarily sinusoids. Subharmonics at 1/3 of the forcing frequency appear that may render the describing function analysis invalid. Note that this case may arise when k_1 and k_2 are chosen using the flux optimization method described earlier.

To analyze the case when subharmonic response is possible, we decompose the plant as shown in Fig. 7 and assume that the linear part of the plant acts as a low-pass filter [15], [16], [17]. For our problem the linear part of the system is

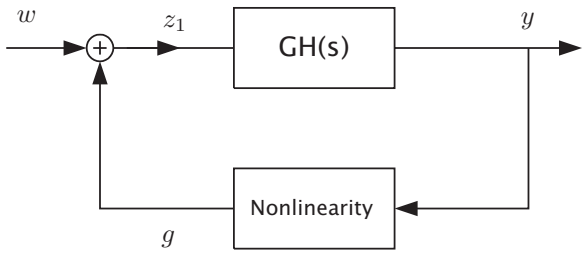

Fig. 7. Block diagram of the AMB model.

$$GH(s) = \frac{-k_1 - k_2 s}{s^2}. \quad (21)$$

The crossover frequency of (21) as a function of the controller gains is easily computed to be

$$\omega_c = \sqrt{\frac{k_2^2 + \sqrt{k_2^4 + 4k_1^2}}{2}}. \quad (22)$$

Let us now analyze the case when the state is *not* sinusoidal.

Figure 8 shows a numerical simulation of the system with a non-sinusoidal response. Figure 9 shows the normalized power spectral densities of the signals at different locations of the block diagram shown in Fig. 7. We notice that the output of the nonlinearity has a major component at the frequency $\omega_0/3$ (ω_0 is the non-dimensional frequency of the speed of rotation and disturbance). Superharmonics at higher frequencies created by the nonlinearity are also present but these are not dominant. After the disturbance

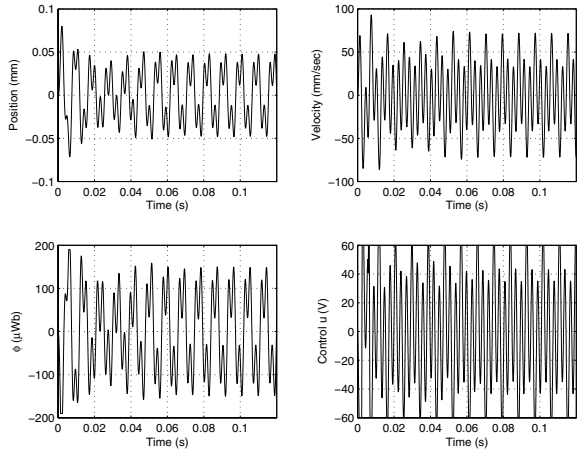

Fig. 8. Example with non-sinusoidal states ($k_1 = 5$, $k_2 = 0.3$, $\Omega_0 = 20,000$ rpm ($\omega_0 = 5.29$), $\Phi_0 = 10\ \mu$Wb, $\gamma = 20$).

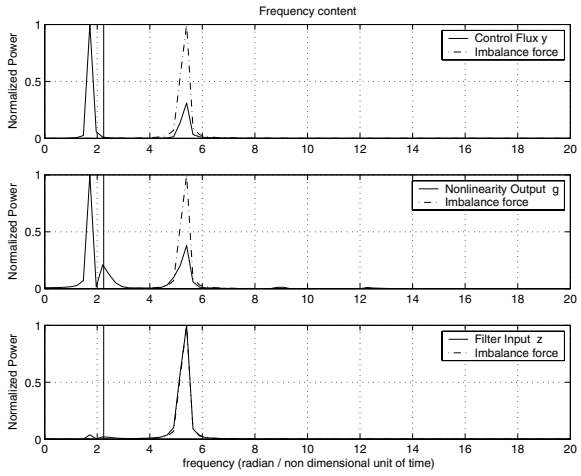

Fig. 9. Normalized power spectral density ($k_1 = 5$, $k_2 = 0.3$, $\Omega_0 = 20,000$ rpm ($\omega_0 = 5.29$), $\Phi_0 = 10\ \mu$Wb, $\gamma = 20$).

(at frequency ω_0) is added at the summation junction, the state z_1, which is the input of the linear part of the system approximates a sinusoid having most of its energy located around ω_0. Nonetheless, some part of the energy is still present at the first subharmonic, at frequency $\omega_0/3$. After the signal passes through the linear system, the part of the signal at frequency $\omega_0/3$ is amplified, but the part of the signal at frequency ω_0 is attenuated. This implies that the cut-off frequency of the linear part of the plant satisfies the inequality $\frac{\omega_0}{3} < \omega_c < \omega_0$.

When this inequality is satisfied, subharmonics may be present. In this case we need to pay a closer attention to the choice of the value of k_1 we pick to compute k_2, or vice versa. To ensure that the subhamonics are not present, we may impose the inequality $\omega_c < \omega_0/3$.

This inequality implies that both harmonics at frequencies ω_0 and $\omega_0/3$ are attenuated. This implies that both k_1 and k_2 are small (cf. (22)). However, the choice of small values for the gains will result in long transient response. On the other hand, if we impose the inequality $\omega_0 < \omega_c$, both harmonics are amplified. In light of (22) and the constraint equation (20), this may not always be possible.

X. Conclusions

Low-bias or zero-bias operation is imperative for minimizing the electromagnetic and ohmic losses of AMBs. Operation at very low-bias requires the use of nonlinear controllers. In this paper, we study the performance of such a nonlinear controller in terms of imbalance rejection. Our approach uses describing functions to replace the nonlinearity with an "equivalent" amplitude-dependent gain. For a given magnitude of position oscillations and a given flux bias, our method allows one to find the controller gains in order to achieve the desired magnitude of position oscillations when the AMB is excited by an imbalance force. Flux saturation is explicitly accounted for. In addition, for a fixed lower bound on the acceptable controller gains, we show how to chose the controller gains to minimize the magnitude of the required flux.

References

[1] M. Aenis and R. Nordman, "Fault diagnosis in rotating machinery using active magnetic bearings," *8th International Symposium on Magnetic Bearing*, 2002, mito, Japan.

[2] M. Anderson and S. Dodd, "Battery energy storage technologies," *Proceedings of the IEEE*, vol. 81, no. 3, pp. 475–479, 1993.

[3] A. Argondizza, B. Aeschlimann, H. Bleuler, S. G. Genta, M. Kummerle, R. Mueller, and A. Tonoli, "FEM based controller design for active magnetic bearings in hard-disk drives," in *Proceedings of the ISROMAC Conference*, 1998.

[4] P. Förch, C. Gähler, and R. Nordmann, "Modal testing in rotating machinery using active magnetic bearings," in *6th International Conference on Vibrations in Rotating Machinery*, 1996.

[5] W. Han, C. Lee, and Y. Okada, "Design and control of a disk type integrated motor-bearing system," *IEEE/ASME Transactions on Mechatronics*, vol. 7, no. 1, pp. 15–22, 2002.

[6] R. Post, T. Fowler, and S. Post, "A high efficiency electromechanical battery," *Proceedings of the IEEE*, vol. 81, no. 3, pp. 470–474, 1993.

[7] Anonymous, "The flywheel revolution," *Electrical Review*, vol. 230, no. 13, pp. 18–20, 1995.

[8] B. Wilson, "Control designs for low-loss active magnetic bearings: Theory and implementation," Ph.D. dissertation, Georgia Institute of Technology, Altanta, GA, March 2004.

[9] A. Gelb and W. E. Vander Velde, *Multiple-Input Describing Functions and Nonlinear system design*. McGraw-Hill Electronic Science Series, 1968.

[10] C. Hayashi, *Nonlinear Oscillations In Physical Systems*. McGraw-Hill Book Company, 1964.

[11] H. P., *Non-Linear Oscillations*. Oxford, England: Clarendon Press, 1981.

[12] H. K. Khalil, *Nonlinear Systems*, 3rd ed. New Jersey: Prentice Hall, 2001.

[13] C. Knospe, "The nonlinear control benchmarck experiment," in *Proceedings of American Control Conference*, 2000, pp. 2134–2138, kobe, Japan.

[14] P. Tsiotras and M. Arcak, "Low-bias control of AMB subject to voltage saturation: State-feedback and observer designs," in *Proceedings, 41st IEEE Conference on Decision and Control*, 2002, pp. 2474–2479, las Vegas, Nevada.

[15] M. A. Aizerman, *Theory of Automatic Control*. Sunderland Technical College, Sunderland: Co. Durham, 1963.

[16] P. Landa, *Nonlinear Oscillations and Waves in Dynamical Systems*. Kluwer Academic Publishers, 1996.

[17] J. Ji and A. Leung, "Non-linear oscillations of a rotor-magnetic bearing system under superhamonic resonance conditions," *International Journal of Non-Linear Mechanics*, vol. 38, no. 6, pp. 829–835(7), 2003.